

1 **Adaptive evolution of *Moniliophthora* PR-1 proteins towards its** 2 **pathogenic lifestyle**

3 Adrielle A. Vasconcelos¹; Juliana José¹; Paulo M. Tokimatu Filho¹; Antonio P. Camargo¹;
4 Paulo J. P. L. Teixeira²; Daniela P. T. Thomazella¹; Paula F. V. do Prado¹; Gabriel L. Fiorin¹;
5 Marcelo F. Carazzolle¹; Gonçalo A. G. Pereira¹; Renata M. Baroni¹

6

7 ¹ Departamento de Genética, Evolução, Microbiologia e Imunologia, Instituto de Biologia,
8 Universidade Estadual de Campinas, Campinas, SP, 13083-862, Brazil.

9 ² Departamento de Ciências Biológicas, Escola Superior de Agricultura “Luiz de Queiroz”
10 (ESALQ), Universidade de São Paulo, Piracicaba, SP, 13418-900, Brazil.

11

12 Corresponding author: goncalo@unicamp.br

13

14 **Abstract**

15 *Moniliophthora perniciosa* and *Moniliophthora roreri* are hemibiotrophic fungi that harbor a
16 large number of Pathogenesis-Related 1 genes, many of which are induced in the biotrophic
17 interaction with *Theobroma cacao*. Here, we provide evidence that the evolution of PR-1 in
18 *Moniliophthora* was adaptive and potentially related to the emergence of the parasitic lifestyle
19 in this genus. Phylogenetic analysis revealed conserved PR-1 genes, shared by many
20 Agaricales saprotrophic species, that have diversified in new PR-1 genes putatively related to
21 pathogenicity in *Moniliophthora*, as well as in recent specialization cases within both species.
22 PR-1 families in *Moniliophthora* with higher evolutionary rates exhibit induced expression in
23 the biotrophic interaction and positive selection clues, supporting the hypothesis that these
24 proteins accumulated adaptive changes in response to host-pathogen arm race. Furthermore,
25 we show that the highly diversified *MpPR-1* genes are not induced by two phytoalexins,
26 suggesting detoxification might not be their main function as proposed before.

27

28 **Introduction**

29 Pathogenesis Related-1 (PR-1) proteins are part of CAP (cysteine-rich secretory
30 proteins, antigen 5, and pathogenesis-related 1) superfamily, also known as SCP/TAPS
31 proteins (sperm-coating protein/Tpx-1/Ag5/PR-1/Sc7), and are present throughout the
32 eukaryotic kingdom (Cantacessi et al., 2009; Gibbs et al., 2008). In plants, PR-1 proteins are
33 regarded as markers of induced defense responses against pathogens (van Loon et al., 2006).

34 These proteins have also been ascribed roles in different biological processes in mammals,
35 insects, nematodes and fungi, including reproduction, cellular defense, virulence and
36 evasion of the host immune system (Asojo et al., 2005; Chalmers et al., 2008; Ding et al., 2000;
37 Gao et al., 2001; Hawdon et al., 1999; Lozano-Torres et al., 2014; Prados-Rosales et al., 2012;
38 Schneider & Di Pietro, 2013; Zhan et al., 2003). In *Saccharomyces cerevisiae*, *Pry* proteins
39 (*Pathogen related in yeast*) bind and export sterols and fatty acids to the extracellular medium,
40 an activity that has also been demonstrated for other proteins of the CAP superfamily through
41 functional complementation assays (Choudhary & Schneider, 2012; Darwiche, Mène-Saffrané,
42 et al., 2017; Darwiche & Schneider, 2016; Gamir et al., 2017; Kelleher et al., 2014).

43 The basidiomycete fungi *Moniliophthora perniciosa* and *Moniliophthora roreri* are
44 hemibiotrophic phytopathogens that cause, respectively, the Witches' Broom disease (WBD)
45 and Frosty Pod Rot of cacao (*Theobroma cacao*). Currently, three biotypes are recognized for
46 *M. perniciosa* based on the hosts that each one is able to infect. The C-biotype infects species
47 of *Theobroma* and *Herrania* (Malvaceae); the S-biotype infects plants of the genus *Solanum*
48 (e.g., tomato) and *Capsicum* (pepper); and the L-biotype is associated with species of lianas
49 (Bignoniaceae), without promoting visible disease symptoms (Evans, 1978; Evans, 2007;
50 Purdy & Schmidt, 1996).

51 With the genome and transcriptome sequencing of the C-biotype, 11 *PR-1*-like genes,
52 named *MpPR-1a* to *k*, were identified in *M. perniciosa* (Teixeira et al., 2012). Interestingly,
53 many of these genes are upregulated during the biotrophic interaction of *M. perniciosa* and *T.*
54 *cacao*, which constitutes a strong indication of the importance of these proteins in the disease
55 process (Teixeira et al., 2012; Teixeira et al., 2014). In this context, efforts have been made to
56 elucidate the role of these molecules during the interaction of *M. perniciosa* with cacao, such
57 as the determination of the tridimensional structure of *MpPR-1i* (Baroni et al., 2017) and the
58 functional complementation of *MpPR-1* genes in yeast *Pry* mutants (Darwiche et al., 2017).
59 These studies revealed that seven *MpPR-1* proteins display sterol or fatty acid binding and
60 export activity, suggesting that they could function as detoxifying agents against plant lipidic
61 toxins (Darwiche et al., 2017).

62 Despite these advances, studies with a deeper evolutionary perspective have not yet
63 been performed for *MpPR-1* proteins. Evolutionary analysis can be an important tool for the
64 inference of gene function and the identification of mechanisms of evolution of specific
65 traits, such as pathogenicity. Genes that are evolving under negative selection pressures are

66 likely to play a crucial role in basal metabolism (Oleksyk et al., 2010). On the other hand, genes
67 that are evolving under positive selection may have changed to adjust their function to a
68 relatively new environmental pressure (Manel et al., 2016). Thus, it can be hypothesized that
69 *Moniliophthora* PR-1 might have accumulated adaptive substitutions in response to selective
70 pressures related to a pathogenic lifestyle, and the analysis of these substitutions may reveal
71 protein targets and specific codons that are potentially important for the pathogenicity in
72 *Moniliophthora*.

73 In this study, we performed a two-level evolutionary analysis of *Moniliophthora PR-1*
74 genes: (i) their macroevolution in the order Agaricales, which consists mainly of saprotrophic
75 fungi, being the *Moniliophthora* species one of the few exceptions; (ii) and their
76 microevolution within *M. pernicioso* and its biotypes that differ in host-specificity. By
77 characterizing PR-1 proteins encoded by 22 *Moniliophthora* genomes, reconstructing their
78 phylogenetic history and searching for evidence of positive selection, we identified an
79 increased diversification in these proteins in *Moniliophthora* that is potentially related to its
80 pathogenic lifestyle, as supported by expression data, and also presents cases of species-
81 specific and biotype-specific diversification.

82

83 **Results**

84

85 **Characterization of PR-1 gene families in *Moniliophthora***

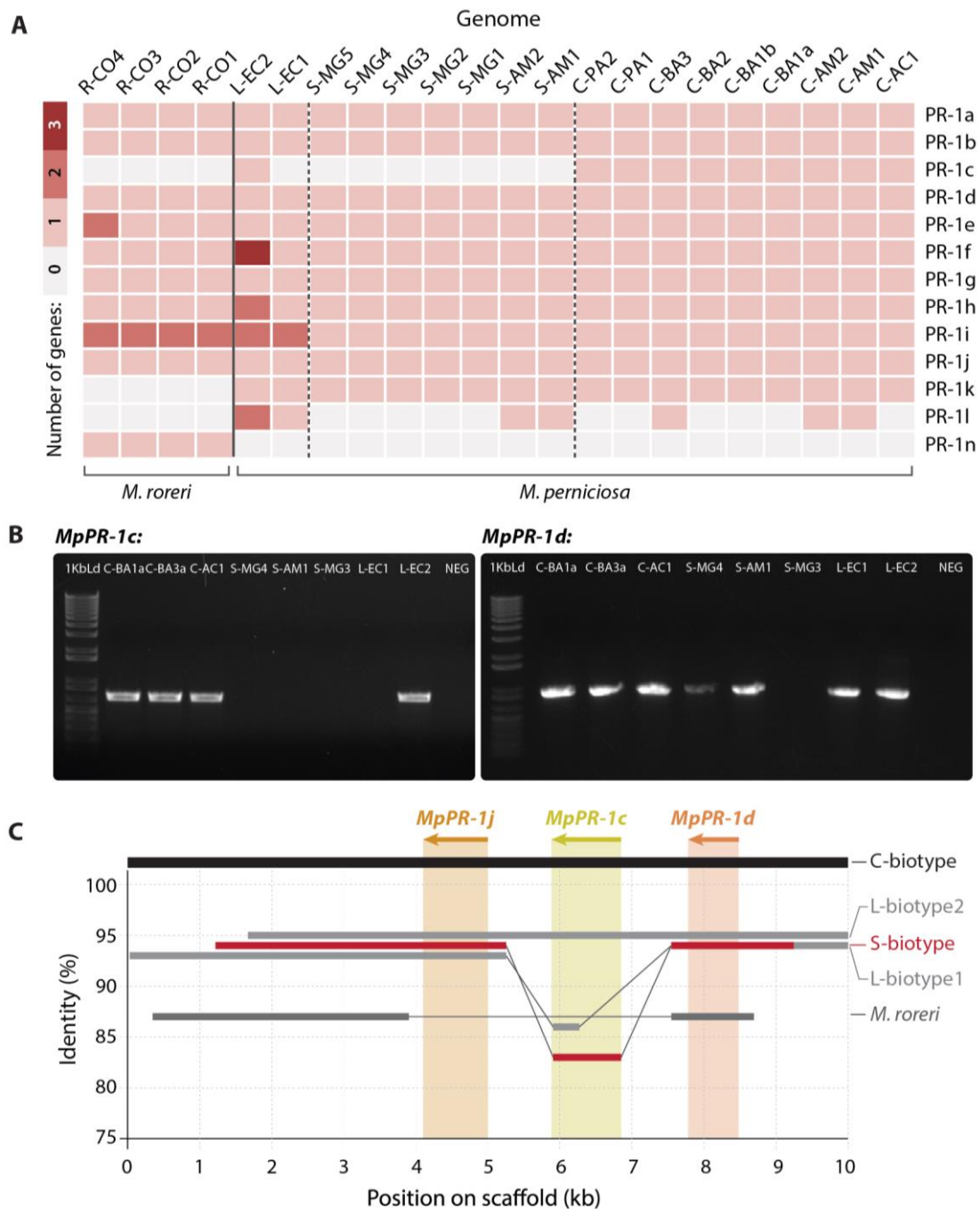
86 Previous work had already reported the identification of 11 PR-1-like genes in the
87 genome of *M. pernicioso* isolate CP02 (C-biotype), which were named *MpPR-1a* to *MpPR-1k*
88 (Teixeira et al., 2012). Likewise, 12 PR-1-like genes were identified in the genome of *M. roreri*
89 (MCA2977) (Meinhardt et al., 2014). With the sequencing and assembly of 18 additional
90 genomes of *M. pernicioso* isolates and other 4 genomes of *M. roreri* isolates, it was possible to
91 characterize the PR-1 gene families in the different biotypes of *M. pernicioso* and in its sister
92 species *M. roreri* in order to look for similarities and differences at the species and biotype
93 levels. Figure 1.A shows the number of genes identified as PR-1 per isolate.

94 The examination of orthogroups containing PR-1-like hits revealed that the PR-1i
95 orthogroup has the highest number of duplications with two copies in *M. roreri* and in L-
96 biotype. Moreover, a new PR-1-like orthogroup with seven candidates that are more similar
97 to *MpPR-1i* (67% identity) was found. This newly identified gene was named “*MpPR-1l*” and

98 was not found in *M. roreri*. It has the same number and structure of introns and exons as the
99 *MpPR-1i* gene and they are closely located in the same scaffold, which is evidence of a
100 duplication event within *M. pernicioso*. Interestingly, the sequences corresponding to *MpPR-*
101 *1l* in the five S-biotype isolates from Minas Gerais were found in another orthogroup, in which
102 *MpPR-1l* was fused to the adjacent gene in the genome (a putative endo-polygalacturonase
103 gene containing the IPR011050 domain: Pectin lyase fold) with no start codon found between
104 the two domains. Furthermore, we found that the *MpPR-1i* gene and, consequently, its
105 predicted protein is truncated in almost all S-biotype isolates from MG (except for S-MG2)
106 (Figure 4).

107 Examining these gene families to look for other putatively species-specific *PR-1* in
108 *Moniliophthora*, we observed that the *MpPR-1k* and *MpPR-1c* genes are not found in the *M.*
109 *roreri* genomes analyzed in this work, while *MrPR-1n* constitutes an exclusive family in this
110 species. The *MrPR-1o* gene previously identified by Meinhardt et al. (2014) was not predicted
111 in any genome as a gene in this work. The protein sequence of *MrPR-1o* has higher identity
112 with *MrPR-1j* (70%), *MpPR-1j* (66%) and *MpPR-1c* (56%), but it is shorter than all 3 protein
113 sequences and does not have a signal peptide like other PR-1 proteins, which suggested that
114 *MrPR-1o* is a pseudogenized paralog of *MrPR-1j*.

115 The absence of *MpPR-1c* in all S-biotype genomes suggested that this gene could be
116 biotype-specific within *M. pernicioso*, however, it was predicted in the L-biotype genome L-
117 EC2. Therefore, we sought to confirm the presence or absence of this gene in different *M.*
118 *pernicioso* by PCR amplification and synteny analysis. The absence of *MpPR-1c* in the S-
119 biotype isolates and in the L-biotype L-EC1 was confirmed, as well as its presence in L-EC2
120 (Figure 1.B). We also amplified the *MpPR-1d* gene, which was predicted in all genomes, in
121 almost all tested isolates, except for S-MG3 because of a mismatch in the annealing regions
122 of both primers. Even though our PCR results indicated that *MpPR-1c* is not present in the S-
123 biotype, synteny analysis of the genome region where *MpPR-1j-c-d* are found in tandem (22)
124 revealed that, in fact, *MpPR-1c* is partially present in these S-biotype genomes (Figure 1.C),
125 suggesting again that the duplication event of PR-1j occurred in the ancestral of *Moniliophthora*
126 but this paralog was also pseudogenized in the evolution of the S-biotype.



127

128 **Figure 1. Characterization of PR-1 gene families in *M. pernicioso* and *M. roseri* genomes. A.**
 129 Heatmap of the number of gene copies per family of PR-1-like candidates per *Moniliophthora*
 130 isolate. Identification of genomes are in columns and PR-1 family names are in rows. **B.**
 131 Amplification by PCR of *MpPR-1c* and *MpPR-1d* genes in the genomic DNA of eight *M.*
 132 *pernicioso* isolates. 1Kb Ld = 1 Kb Plus DNA Ladder (Invitrogen), Neg = PCR negative control
 133 (no DNA). Expected fragment sizes were 687 bp for *MpPR-1c* and 902 bp for *MpPR-1d*. **C.**
 134 Synteny analysis of a 10 Kb portion of the genome where the *MpPR-1j*, *c*, *d* genes are found in
 135 the three biotypes of *M. pernicioso* and *M. roseri*. The genomes analyzed were C-BA3, S-MG2,
 136 R-CO2, L-EC1 and L-EC2. Only identity above 75% to the C-biotype reference is shown.

137

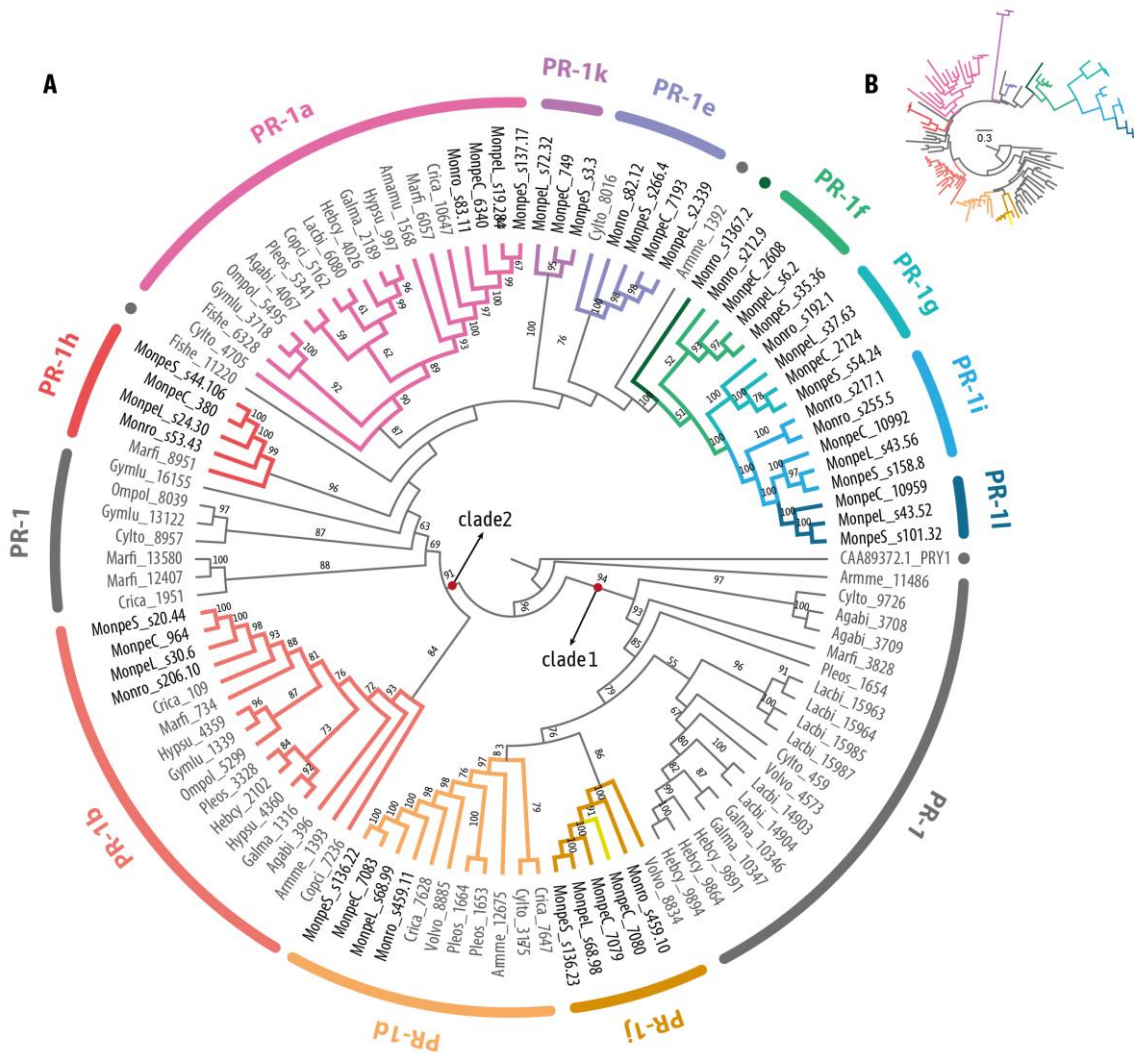
138 **PR-1 genes evolution along the Agaricales order**

139 To study the macroevolution of PR-1 proteins, we identified orthologous sequences of
140 genes encoding PR-1-like proteins in 16 genomes of species from the Agaricales order,
141 including 3 selected *M. pernicios*a genomes (one of each biotype) and 1 *M. roreri* genome for
142 comparisons. The phylogenetic reconstruction of Agaricales PR-1 proteins revealed a basal
143 separation of two major clades, hereafter called clade1 and clade2 (Figure 2.A).

144 The first PR-1 clade includes most Agaricales species outside *Moniliophthora* showing
145 *PR-1* genes that diverged early in the phylogeny, before the appearance of PR-1a-l-n
146 orthologues. From this first clade including the early diverged PR-1 proteins, subsequently
147 diverged PR-1d and PR1-j. The separation between PR-1d and j proposed for *Moniliophthora*
148 only occurs in *Volvarella volvacea*, while for all other species, paralogous of PR-1d diverged
149 early. In *Moniliophthora*, PR-1j and PR-1d have more recent common ancestors, and the only
150 paralogous of these *Moniliophthora* PR-1s originates from a possible duplication of *MpPR-1j*
151 in the C-biotype of *M. pernicios*a, which was previously named *MpPR-1c*, therefore exclusive
152 to this species and biotype.

153 The second clade includes all other PR-1 families and other Agaricales PR-1s that do
154 not have a common ancestor with a single PR-1 from *Moniliophthora*. Clade2 is divided into 2
155 subclasses in its base, one of them composed of the PR-1b clade, which is distributed among
156 14 species. In the second subgroup, PR-1a shows a common ancestor in a total of 16 species,
157 being the most common PR-1 here. The great diversification of a PR-1a-like ancestor in
158 *Moniliophthora* resulted in the formation of at least 4 new and exclusive *PR-1* genes (*k*, *g*, *i*, *l*)
159 with high evolutionary rates reflected on the branch lengths (Figure 2.B). PR-1n showed a
160 putative ortholog in *Armillaria mellea*, the only other plant pathogen in the Agaricales dataset,
161 however, this connection has low branch support.

162



163

164

Figure 2. Phylogenetic cladogram of PR-1 proteins in Agaricales (Basidiomycota).

165

Phylogenetic relationships were inferred by maximum likelihood and branch support was

166

obtained using 1000 bootstraps. Only branch support values greater than 70 are shown. PR-1c

167

is indicated as a yellow branch inside the PR-1j clade, and PR-1n is indicated with a dark green

168

dot and branch. Proteins with ancestral divergence to more than one family were named with

169

the letters of the derived families. Full species names are in SM1. The branch lengths were

170

dimensioned for easy visualization. **B.** The same phylogeny shown in “A” is presented with

171

the respective branch lengths augmented for the *Moniliophthora* specific PR-1 genes.

172

173

Recent diversification of PR-1 genes in *Moniliophthora*

174

Through the investigation of the phylogenetic history of PR-1 proteins within 22

175

Moniliophthora isolates (Figure 3), we found that the previous classification of *MpPR-1a* to *k*

176

and *MrPR-1n* represents monophyletic clades in the tree, except for *MpPR-1c* which is a recent

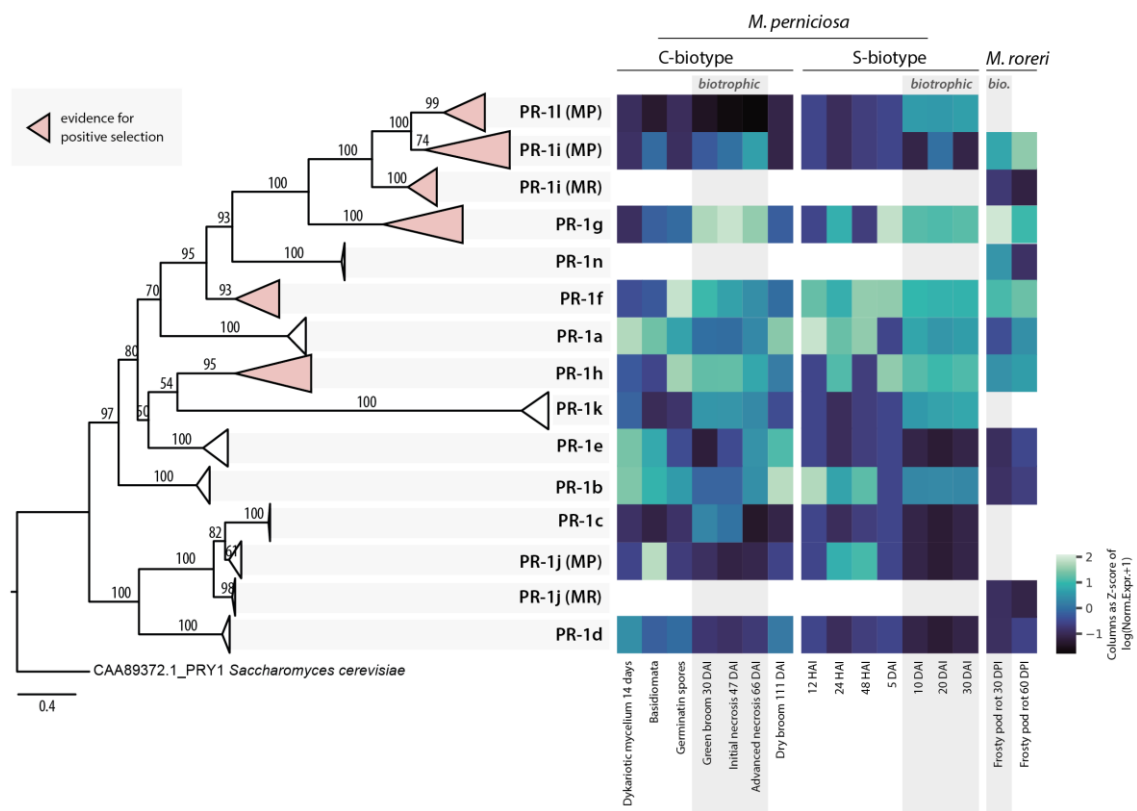
177

paralogous of *MpPR-1j*. The evolution of *Moniliophthora* PR-1 also reflected the basal

178 divergence between two large clades as observed in the Agaricales PR-1 tree (Figure 2). The
 179 only incongruence between the two phylogenetic trees is the relative position of PR-1k, which
 180 appeared after the divergence of PR-1a in Agaricales and before it in *Moniliophthora*. This
 181 incongruence may be due to the extreme differentiation of PR-1k, with longer branch lengths
 182 in *Moniliophthora*, being its position on the Agaricales tree more reliable.

183 Among the PR-1 families, the proteins with the greatest number of changes in the tree
 184 are PR-1g, i, and k, which are exclusive PR-1s in the genus *Moniliophthora*, as pointed out by
 185 the previous phylogenetic analysis. In addition, PR-1h also showed a greater branch length
 186 than the others, being a family of PR-1s only shared between *Moniliophthora* and *Marasmius*
 187 in the Agaricales PR-1 tree (Figure 2). PR-1c also presented a large number of changes in
 188 relation to its ancestor PR-1j. This greater number of changes in these MpPR-1s, and their
 189 exclusive presence in comparison to the other Agaricales, indicate a recent potential adaptive
 190 process of diversification of these proteins in *Moniliophthora*.

191



192

193 **Figure 3. Phylogenetic reconstruction of PR-1 proteins in *Moniliophthora* and heatmap of**
 194 **expression Z-scores of PR-1.** Phylogenetic relationships of PR-1 proteins from 18 *M.*
 195 *pernicioso* and 4 *M. roreri* isolates were inferred by maximum likelihood and branch support
 196 was obtained using 1000 bootstraps. The PRY1 protein of *Saccharomyces cerevisiae* was used as

217 an outgroup. Clades filled with pink color represent PR-1 families with evidence of positive
218 selection. A version of this tree with non-collapsed branches can be found in Supplementary
219 Figure 1. For each PR-1 family, the Z-score of log transformed expression levels of *MpPR-1*
220 and *MrPR-1* from transcriptomic data was calculated for conditions (columns) and plotted as
221 a heatmap. The heatmap includes *MpPR-1* data from seven conditions of the C-biotype of *M.*
222 *perniciosa* from the Witches' Broom Transcriptomic Atlas, 7 different time points of S-biotype
223 infection in MicroTom tomato plants, and two conditions of *M. roreri* infection in cacao pods
224 (frosty pod rot). Conditions highlighted with a grey background indicate the biotrophic stage
225 of the plant-pathogen interaction.

226

227 **Positive selection shaping PR-1 families in *Moniliophthora***

228 Based on the observations of high diversification of PR-1 families within
229 *Moniliophthora*, we hypothesized that positive selection could be shaping these proteins
230 either in the C-biotype or in the S-biotype. To test this hypothesis, we tested the branch-sites
231 evolutionary model for each PR-1 family. None of these tests brought evidence of positive
232 selection in any PR-1 family for the C-biotype branches. For the S-biotype branches, a signal
233 of positive selection was detected for PR-1g on one site of the protein sequence.

234 Considering that the existence of *M. perniciosa* biotypes are very recent in the
235 evolutionary timescale and that C-biotype itself has almost no genetic variation among its
236 sequences, which makes it very difficult to apply separate dN/dS tests, we tested both C- and
237 S- biotypes together. We tested the hypothesis that there was a single selective pressure
238 shaping PR-1 families throughout the *M. perniciosa* and *M. roreri* evolution regardless of the
239 biotype, using the site model test. In these tests, sites with positive selection signs were
240 detected in five families (PR-1f, g, h, i, l) (Table 2). The PR-1n family was not included in these
241 tests because all sequences were identical.

242 PR-1g stands out for having the highest omega and for being one of the most expressed
243 genes during the green broom phase (Teixeira et al., 2014). Three of the codons under positive
244 selection are part of the 'keke' domain, which is possibly involved in the interaction with
245 divalent ions or proteins (Teixeira et al., 2012). Among the sites detected under positive
246 selection for PR-1i, one is found in the caveolin binding motif (CBM), an important region for
247 binding to sterols, and another site is in the alpha-helix 1, which together with alpha-helix 4
248 form the cavity for ligation to palmitate (Baroni et al., 2017) (Figure 4).

249 Although the two exclusive PR-1 families of *M. perniciosa*, PR-1c and PR-1k, do not
250 present evidence of positive selection, both revealed processes of diversification in the PR-1

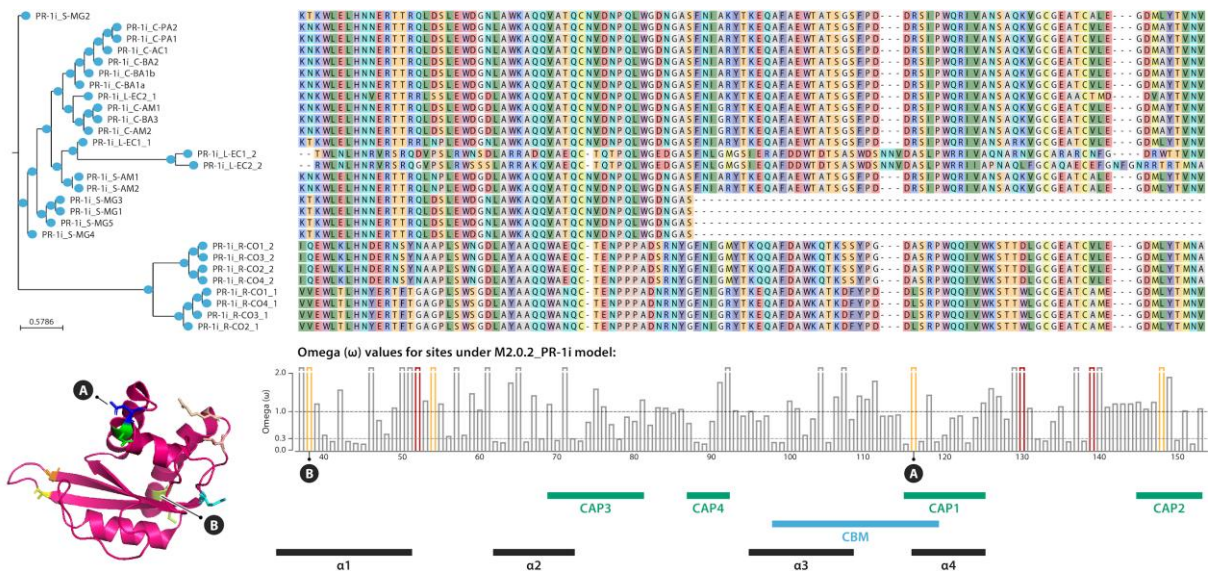
231 phylogenies. It is possible that these families have also undergone selective pressures in their
 232 evolution, but the short time of evolution of *M. perniciososa* in relation to the genus has reduced
 233 the accuracy of the dN/dS tests in these exclusive families.

234

235 **Table 2.** Omega (dN/dS) values and protein sites (amino acid: position) detected with
 236 significant probability of positive selection for each PR-1 family in *Moniliophthora*.

Family	Omega	Sites under positive selection (p>0.95)
PR-1a	4.12	None
PR-1b	2.31	None
PR-1c	1	None
PR-1d	2.07	None
PR-1e	1	None
PR-1f	2.74	K: 49, S: 157
PR-1g	7.05	P: 211, P: 234, A: 242, S: 260, S: 271
PR-1h	4.33	S: 78, Y: 107, P: 141, S: 155, E: 187, D: 206, L: 209, M: 224, R: 259, Q: 267
PR-1i	4.38	T: 40, Q: 54, D: 56, R: 118, K: 132, A: 141, L: 150
PR-1l	6.39	Q: 65, Q: 76, -: 164, N: 176, R: 192, K: 193, E: 194, F: 196
PR-1j	2.76	None
PR-1k	2.50	None

237



238

239 **Figure 4. Sequence alignment and phylogeny of PR-1i proteins in *Moniliophthora* isolates.**

240 Only a slice of the middle portion of the alignment is shown to highlight the sites with positive
 241 selection signs, indicated by red (p-value ≤ 0.01) or orange (p-value ≤ 0.05) bars in the bar
 242 chart of omega values below the alignment. Below de bar chart, annotations indicate the
 243 locations along the sequence of the CAP domains, caveolin-binding motif (CBM) and alpha-

244 helices (α). On the 3D crystal structure of MpPR-1i protein (PBD:5V50) and on the bar chart,
245 “A” indicates the site under positive selection detected in the CBM and “B” indicates the site
246 under positive selection in alpha-helix 1.

247

248 **Adaptive evolution of PR-1 is reflected on expression data**

249 It has already been shown that *MpPR-1* genes of the C-biotype have distinct expression
250 profiles in several different conditions of the WBD Transcriptome Atlas, which were also
251 confirmed by quantitative RT-PCR (Teixeira et al., 2012; Teixeira et al., 2014). *MpPR-1a, b, d,*
252 *e* are ubiquitously expressed during the necrotrophic mycelial stage, while *MpPR-1j* is mainly
253 expressed in primordia and basidiomata. Six *MpPR-1s* are highly and almost exclusively
254 expressed during the biotrophic stage of WBD: *MpPR-1c, f, g, h, i, k* (Teixeira et al., 2012).
255 However, in contrast to *MpPR-1i*, the newly discovered *MpPR-1l* is not expressed in any of the
256 conditions analyzed, suggesting that this gene may not be functional in the C-biotype.

257 Expression data of *MpPR-1* genes from the S-biotype during a time course of the
258 biotrophic interaction with MT tomato revealed that *MpPR-1f, g, h, l,* and *k* are highly
259 expressed during 10-30 days after infection (d.a.i.) (Figure 3). These results are similar to the
260 expression profile verified for the C-biotype during the biotrophic interaction with *T. cacao*,
261 with the exceptions that *MpPR-1c* is absent in the S-biotype and, instead of *MpPR-1i*, *MpPR-1l*
262 is expressed during tomato infection. S-biotype *MpPR-1s* are highly expressed starting at 10
263 d.a.i., which is usually when the first symptoms of stem swelling are visible in MT tomato
264 (Deganello et al., 2014). *MpPR-1a* and *b* appear to have ubiquitous expression profiles since
265 they show similar expression levels in almost all conditions. *MpPR-1j, d, e,* and *i* did not show
266 significant expression in these libraries. Because *MpPR-1i* is truncated in the S-MG1 genome,
267 quantification of expression was also done with S-MG2 as a reference, since it has a complete
268 *MpPR-1i* gene. However, we still obtained the same expression profiles as S-MG1 for all *MpPR-*
269 *1*. This could suggest that *MpPR-1l* is expressed in S-biotype even with a fusion to the adjacent
270 gene. In the C-biotype, this adjacent gene is only expressed during the biotrophic interaction.

271 In *M. roreri*, it has been previously reported that *MrPR-1n, MrPR-1g* and *MrPR-1i2*
272 were upregulated in samples from the biotrophic phase (30 days post infection of pods),
273 *MrPR-1d* was upregulated in the necrotrophic phase (60 days post infection of pods) and five
274 other *MrPR-1* were constitutively expressed under these conditions (Meinhardt et al., 2014).
275 The heatmap in Figure 3 shows that similar to *M. pernicioso's* PR-1 expression profile, *MrPR-*

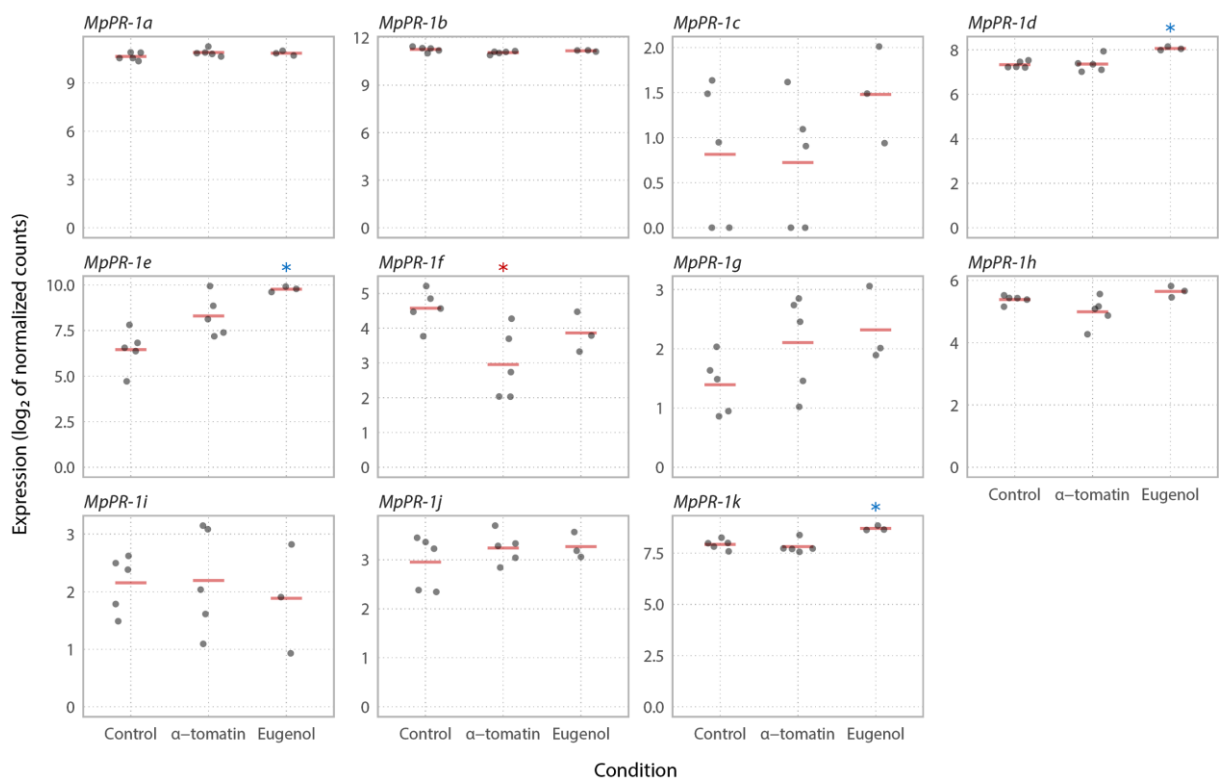
276 *Ig* is the most expressed *PR-1* gene during the biotrophic stage. Moreover, while *MrPR-1h* and
277 *MrPR-1f* were not differentially expressed when comparing the biotrophic and necrotrophic
278 stages, they also showed higher expression when compared to other *MrPR-1s* that belong to
279 the conserved families.

280

281 **Expression of recently diversified MpPR-1 was not induced by plant antifungal** 282 **compounds**

283 It has been previously demonstrated that CAP proteins of *M. perniciosa* bind to a
284 variety of small hydrophobic ligands with different specificities. Thus, it has been suggested
285 that the *MpPR-1* genes induced in the biotrophic interaction could function in the
286 detoxification of hydrophobic molecules produced by the host as a defense strategy
287 (Darwiche et al., 2017). In this context, we investigated if *MpPR-1* genes, especially the ones
288 induced in WBD (*c, f, h, i, k, g*), are differentially expressed by the presence of the plant
289 antifungal compounds eugenol or α -tomatin, which are similar to sterol and fatty acids,
290 respectively. However, when the necrotrophic mycelia of *M. perniciosa* was treated with
291 eugenol, only *MpPR-1e, k, d* were up-regulated, while *MpPR-1f* was down-regulated in α -
292 tomatin-treated samples (Figure 5). In all samples, among all *MpPR-1* genes, *MpPR-1a* and
293 *MpPR-1b* had the highest expression levels, while *MpPR-1c, i, g, j* have the lowest (TPM ≤ 2).

294



295

296 **Figure 5. Expression profile of *MpPR-1* genes in response to two plant antimicrobial**
297 **compounds.** The necrotrophic mycelium of *M. pernicioso* C-biotype (C-BA1a) was grown in
298 liquid media in the presence of eugenol, α -tomatin or DMSO (mock condition) for 7 days. The
299 expression values (Log2 transformed) for each *MpPR-1* were obtained by RNA-Seq and
300 subsequent quantification of read counts and between-sample normalization using size
301 factors. Red bars indicate the mean of expression values within a group of replicates.
302 Asterisks indicate that *MpPR-1e*, *k*, *d*, *f* are differentially expressed (s-value<0.005) when
303 compared to the mock condition, with blue asterisk indicating up-regulation and red
304 indicating down-regulation.
305

306 Discussion

307 The evolution of PR-1 and the emergence of pathogenicity among saprotrophs

308 The plant pathogen *M. pernicioso* has at least 11 genes encoding PR-1-like secreted
309 proteins, which were previously identified and characterized in the genome of the C-biotype
310 CP02 isolate (Teixeira et al., 2012). Many of these genes were shown to be highly expressed
311 during the biotrophic interaction of *M. pernicioso* and cacao, suggesting that MpPR-1 proteins
312 have important roles during this stage of WBD. *M. pernicioso* has two other known biotypes (S
313 and L) that differ in host specificity and virulence, the closest related species *M. roreri* that
314 also is a *T. cacao* pathogen, and other nine *Moniliophthora* species: one described as a non-
315 pathogenic grass endophyte (Aime & Phillips-Mora, 2005), three of biotrophic/parasitic habit
316 (Niveiro et al., 2020), and five species of unascertained lifestyle, found in dead or decaying
317 vegetal substrates (Kerekes et al., 2009; Kropp & Albee-Scott, 2012; Takahashi, 2002). Because
318 the majority of *Moniliophthora* related fungi in the Agaricales order are saprotrophs, the
319 occurrence of parasitic *Moniliophthora* species raises the question about the emergence of
320 biotrophic/parasitic lifestyle in this lineage of Marasmiaceae (Niveiro et al., 2020; Teixeira et
321 al., 2015). The evolutionary scenario of host-pathogen arms race that emerges through the
322 diversification of the *Moniliophthora* genus in the Agaricales order and of host-specific
323 biotypes in *M. pernicioso* isolates, is especially suitable for the study of adaptive evolution in
324 pathogenicity-related genes. Besides, the knowledge on putative adaptations gained through
325 pathogen evolution are also specially interesting for further development of strategies against
326 the pathogen. Based on our findings, Figure 6 presents a model for the adaptive evolution of
327 PR-1 proteins in *Moniliophthora*.

328 Through the characterization of the evolution of PR-1 proteins in Agaricales, we
329 observe that at least one copy of PR-1 is present in all the sampled fungi, with most of the

330 Agaricales species encoding between 1 and 7 PR-1 proteins. This is in contrast with
331 *Moniliophthora* species, which encode among 10-12 proteins. *Moniliophthora* PR-1 proteins
332 are derived independently from both ancient clades in the Agaricales gene tree. The longer
333 branch-lengths in PR-1 families exclusive to *Moniliophthora* along with the evidence of
334 evolution under positive selection identified in independently diverged clades suggest that
335 the diversification of PR-1 in the genus was adaptive and related to its pathogenic lifestyle.
336 The accentuated adaptive evolution of PR-1 in *Moniliophthora* is not only reflected in the
337 genomic evolution of these genes, but also in their expression context. *PR-1c, f, g, h, i, k, l, n*
338 are upregulated during the biotrophic interaction, while *PR-1s* that are also conserved in
339 other Agaricales species are mainly expressed in mycelial stages of *M. perniciosa* (*MpPR-1a,*
340 *b, d, e*). Most Agaricales species are not plant pathogens, which is also an evidence that PR-1
341 in *Moniliophthora* diverged from a few ancestral PR-1s that are related to basal metabolism in
342 fungi and have been evolving under positive selective pressure possibly because of a benefit
343 for the biotrophic/pathogenic lifestyle.

344 The emergence of SCP/TAPs proteins as pathogenicity factors has been reported in
345 other organisms, such as the yeast *Candida albicans* and the filamentous fungus *Fusarium*
346 *oxysporum* (Braun et al., 2000; Prados-Rosales et al., 2012). Even though their specific function
347 and mode of action may be different and remains to be characterized in plant pathogens, the
348 recent evolution of these proteins towards their pathogenic role in the *Moniliophthora* genus
349 could have contributed for the transition from a saprotrophic to parasitic lifestyle.
350 Accelerated adaptive evolution evidenced by positive selection signs has also been observed
351 in other virulence-associated genes of pathogenic fungi, such as the genes *PabaA, fos-1, pes1,*
352 and *pksP* of *Aspergillus fumigatus*, which are involved in nutrient acquisition and oxidative
353 stress response (Fedorova et al., 2008), and several gene families in *C. albicans*, including cell
354 surface protein genes enriched in the most pathogenic *Candida* species (Butler et al., 2009).

355

356 **Adaptive evolution of PR-1 within *Moniliophthora* species and its biotypes**

357 The high diversification of PR-1 families observed within *Moniliophthora* was
358 reinforced by our findings of positive selection in families that have also augmented
359 expressions during infection: PR-1f, g, h, i, l. Among these five families, PR-1g and PR-1i are
360 two of the most diversified families in *Moniliophthora* and have a more recent common
361 ancestor with PR-1f than with the other PR-1s, placing this monophyletic clade of PR-1f, g, i
362 as the key one to diversification and adaptive evolution of these proteins in the genus. Many

363 sites that potentially evolved under selective pressure were also found in PR1-h, indicating
364 that a parallel process of adaptive evolution occurred in this family.

365 Within the diversification of PR-1 in *Moniliophthora*, four cases of putative species-
366 specific evolution of PR-1 families were found: PR-1c, PR-1k and PR-1l in *M. pernicioso* and
367 PR-1n in *M. roreri*. Although vestigial sequences indicate that PR-1c probably emerged as a
368 paralog of PR-1j in the ancestral of both species, it was only kept in the evolution of C-biotype,
369 in which a change in expression profile occurred, thus placing *MpPR-1c* as a case of PR-1
370 diversification within *M. pernicioso* biotypes and a potential candidate for host specificity.
371 Another candidate for biotype-specific diversification is PR-1l, which diverged from a
372 duplication of PR-1i. Even though PR-1l was found in all three *M. pernicioso* biotypes, it was
373 expressed only in the S-biotype during the biotrophic interaction, instead of PR-1i, which is
374 expressed in *M. roreri* and in the C-biotype. This suggests that the divergence of PR-1i can be
375 host-specific, but further experiments are necessary to clarify if they are either a cause or
376 consequence of *M. pernicioso* pathogenicity.

377 Even though almost all PR-1 families are present in the genomes of L-biotype isolates,
378 this biotype has an endophytic lifestyle and does not cause visible disease symptoms in their
379 hosts (H. C. Evans, 1978; Griffith & Hedger, 1994). There is no available expression data for
380 the L-biotype, so it is unknown whether their PR-1 genes could have any role related to their
381 lifestyle or these genes are not pseudogenized yet due to a small evolutionary time. Evans
382 (1978) reported that the L-biotype can induce weak symptoms in seedlings of the Catongo
383 variety of *T. cacao*. Therefore, it could be possible that host susceptibility is an important
384 factor for the manifestation of WBD symptoms.

385

386 **From basal metabolism to key roles in disease: How PR-1 proteins could have** 387 **functionally adapted for pathogenicity?**

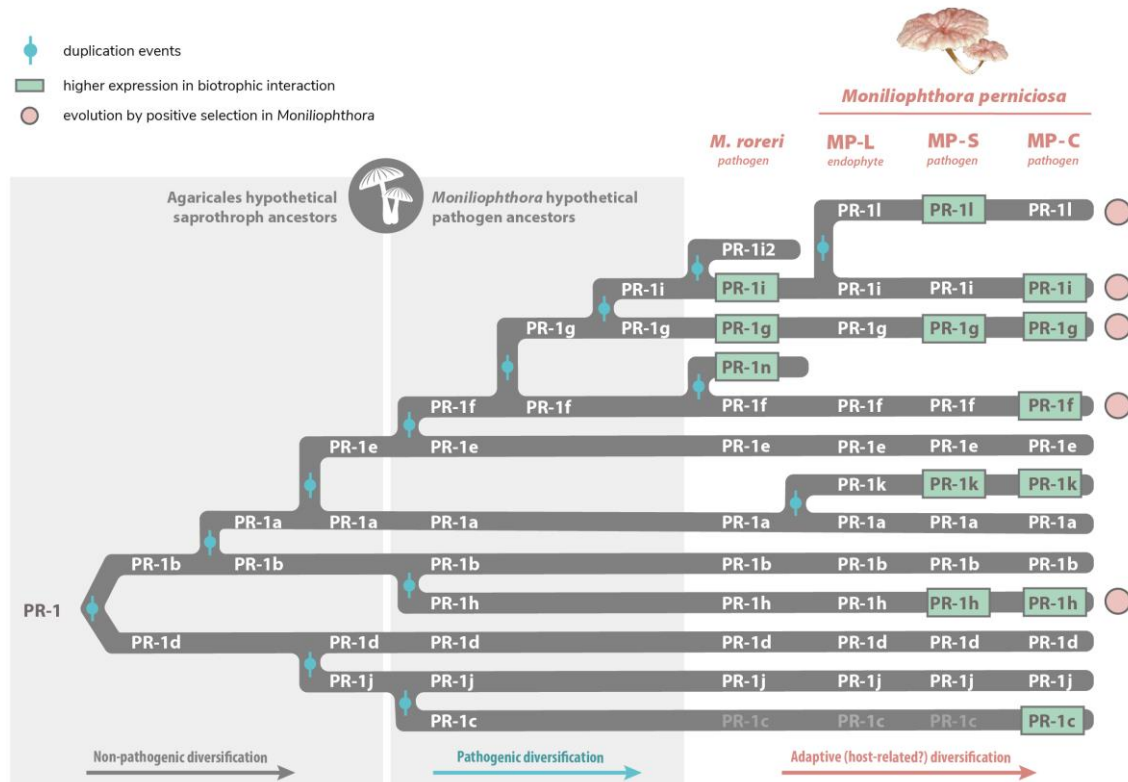
388 It was previously shown that Pry proteins detoxify and protect yeast cells against
389 eugenol (Darwiche, Mène-Saffrané, et al., 2017) and that *MpPR-1* proteins can bind to
390 hydrophobic compounds secreted by plants, indicating that they could antagonize the host
391 defense response (Darwiche, El Atab, et al., 2017). When the necrotrophic mycelia of *M.*
392 *pernicioso* was cultivated with eugenol, expression of *MpPR-1d* and *MpPR-1k* was up-
393 regulated, which is in agreement with the ability of these two proteins to bind to plant and
394 fungal sterol compounds (Darwiche, El Atab, et al., 2017). *MpPR-1e* expression was also highly

395 induced by eugenol, even though it was previously shown to bind only to fatty acids, but not
396 sterols. Additionally, *MpPR-1f*, which is up-regulated during the biotrophic interaction like
397 *MpPR-1k*, was down-regulated by α -tomatin. Given the above, it appears that *M. pernicioso*
398 does not rely on MpPR-1 for cellular detoxification or this function is not transcriptionally
399 regulated by plant hydrophobic compounds in the necrotrophic mycelia, or even, they could
400 have different roles other than detoxification.

401 Considering that some PR-1 proteins are not associated with infection and are
402 conserved in other saprotrophic fungi, here we hypothesize that the primary function of PR-
403 1 in fungi can be related to the export of sterols from basal metabolism, such as ergosterol,
404 the most abundant sterol in fungal cell membrane (Mohd et al., 2011; Zhao et al., 2005). PRY
405 of *S. cerevisiae* transports acetylated ergosterol to the plasma membrane (Choudhary &
406 Schneider, 2012) and MpPR-1d, which belongs to a relatively conserved PR-1 family in
407 Agaricales, can also efficiently bind to ergosterol (Darwiche et al., 2017). Furthermore,
408 ergosterol acts as a PAMP molecule (pathogen-associated molecular pattern) in plants
409 (Nürnberg et al., 2004), resulting in the activation of defense-related secondary metabolites
410 and genes, including plant PR-1s (Kasparovsky et al., 2003; Klemptner et al., 2014; Lochman
411 & Mikes, 2006; van Loon et al., 2006), which are likely to have a role in sequestering sterols
412 from the membranes of microbes (Gamir et al., 2017) and stress signaling (Chen et al., 2014;
413 Chien et al., 2015). Additionally, PR-1 receptor-like kinases (PR-1-RLK) from *T. cacao* are also
414 upregulated on WBD and could be binding to the same ligand of PR-1 (Teixeira et al., 2013).
415 Given that, it is possible that MpPR-1 could have evolved different adaptive roles through
416 neofunctionalization. Besides export of hydrophobic compounds of basal metabolism, they
417 could be acting in the protection of the cell membrane against the disruption caused by
418 antifungal compounds, in the detoxification of hydrophobic compounds like phytoalexins
419 secreted by the host, or it could even be possible that those *MpPR-1s* expressed during
420 infection are sequestering the membrane sterols of the fungus itself in order to prevent
421 detection by a possible ergosterol recognition complex from the host (Khoza et al., 2019), thus
422 compromising the elicitation of plant immunity in a similar fashion of MpChi, a chitinase-
423 like effector that is highly expressed by *M. pernicioso* during the biotrophic stage of WDB
424 (Fiorin et al., 2018).

425 It has been shown that the ability of MpPR-1 proteins to bind to sterols can be altered
426 by a point mutation in the caveolin binding motif (Darwiche et al., 2017), highlighting the
427 significance of understanding those sites under positive selection that are detected in

428 important regions of the proteins, such as the candidate sites found in the CBM and alpha-
 429 helix 1 of PR-1i. These findings are central to learn how changes in the nucleotide or protein
 430 sequences could impact binding affinity and function. Even though this is speculative, as the
 431 specific role of PR-1 remains unknown, these results can guide further validation
 432 experiments and maybe demonstrate another case of adaptive evolution of fungal effectors.
 433



434
 435 **Figure 6. Proposed model for the adaptive evolution of PR-1 proteins in *Moniliophthora***
 436 **towards the pathogenic lifestyle.** All *Moniliophthora* PR-1 proteins derived independently
 437 from two ancient clades (PR-1b-like and PR-1d-like) within the Agaricales order, as indicated
 438 in PR-1 phylogeny. The subsequent diversification of PR-1a and PR-1e from PR-1b, and PR-1j
 439 from PR-1d, occurred in putative saprotroph lineages before the divergence of *Moniliophthora*
 440 genus, suggesting a diversification not related to pathogenicity. Within *Moniliophthora*
 441 hypothetical pathogenic ancestors, five other PR-1 proteins were derived (c from j, h from b,
 442 f-g-i from e) and most of these new lineages showed evidence of positive selection in *M.*
 443 *perniciosa* samples (indicated by pink circles). New PR-1 copies (n and i2 in *M. roreri*, l and k
 444 in *M. perniciosa*) diverged within *M. perniciosa* species. Recently diversified PR-1 genes in
 445 *Moniliophthora*, not only show an elevated rate of evolution and positive selection evidence
 446 but are also predominantly expressed during the biotrophic interaction (indicated by green
 447 highlights). This supports the hypothesis that these proteins accumulated adaptive changes
 448 related to pathogen lifestyle that might also contribute to the host specialization observed in
 449 *Moniliophthora* species and biotypes.
 450

451 **Conclusions**

452 Based on genomic and transcriptomic data, we presented evidence of adaptive
453 evolution of PR-1 proteins in processes underlying the pathogenic lifestyle in *Moniliophthora*.
454 These results reinforce the power of evolutionary analysis to reveal key proteins in the
455 genomes of pathogenic fungi and contribute to the understanding of the evolution of
456 pathogenesis. Our results indicate a set of PR-1 families that are putatively related to
457 pathogenicity in the genus (PR-1f, g, h, i) and specialization within *M. pernicioso* biotypes (PR-
458 1c, k and l) and *M. roreri* (PR-1n). The positive selection analysis also indicates protein sites
459 that are putatively related to those adaptations. *PR-1* genes and sites with evidence of
460 adaptations are strong candidates for further study and should be evaluated in order to
461 understand how changes in these sites can affect structure, binding affinity and function of
462 these proteins.

463

464 **Material and Methods**

465

466 **Identification of PR-1-like gene families**

467 In this study, we used a dataset of families of genes predicted in 22 genomes of
468 *Moniliophthora* (unpublished) and 16 genomes of other fungal species of the order Agaricales,
469 which were obtained from the Joint Genome Institute (JGI) Mycocosm database (Grigoriev et
470 al., 2014). The *Moniliophthora* genomes included are 7 isolates of the S-biotype (collected at
471 the states of Amazonas and Minas Gerais, in Brazil), 9 isolates of the C-biotype (collected at
472 the states of Amazonas, Pará, and Acre, in Brazil), 2 isolates of the L-biotype (from Colombia)
473 and 4 samples of *M. roreri* (from Colombia). Supplementary Table 1 contains the list of species
474 and isolates, their genome identification and source (collection location or reference
475 publication).

476 To identify candidate *PR-1* gene families, we performed a search for genes encoding
477 the CAP/SCP/PR1-like domain (CDD: cd05381, Pfam PF00188) using the HMMER software
478 (Eddy, 2011). The assignment of protein sequences to families of homologues (orthogroups)
479 was done using Orthofinder (v. 1.1.2) (Emms & Kelly, 2015). In addition, we searched all gene
480 families for families containing *PR-1* candidate genes with Blastp (Camacho et al., 2009) using
481 the known 11 MpPR-1 sequences (Teixeira et al., 2012) as baits, in order to search for possible
482 candidates that were not previously identified and/or that have been wrongly assigned to

483 other orthogroups due to incorrect gene prediction. To verify the presence of the SCP PR1-
484 like/CAP domain (InterPro entry IPR014044) in the sequence, the InterProscan platform
485 (Hunter et al., 2009) was used. All PR-1 candidate sequences identified in this study are
486 deposited in GenBank under accession numbers MW659198 - MW659445.

487

488 **Sequence alignment and phylogenetic reconstruction**

489 For the inference of the phylogenetic history of the gene, the protein sequences of the
490 PR-1 homologue families identified in the 22 *Moniliophthora* isolates were aligned with the
491 PRY1 sequence of *S. cerevisiae* (GenBank ID CAA89372.1), which was used as outgroup.
492 Multiple sequence alignments were performed with Mafft (v. 7.407) (Katoh & Standley, 2013)
493 using the iterative refinement method that incorporates local alignment information in pairs
494 (L-INS-i), with 1000 iterations performed. Then, the alignments were used for phylogenetic
495 reconstruction using the maximum likelihood method with IQ-Tree (v. 1.6.6) (Nguyen et al.,
496 2015), which performs the selection of the best replacement model automatically, with 1000
497 bootstraps for branch support. Bootstraps were recalculated with BOOSTER (v. 0.1.2) for
498 better support of branches in large phylogenies (Lemoine et al., 2018). Likewise, the
499 phylogenetic inference for PR-1 of the Agaricales group of species was performed with the
500 alignment of the homologous proteins identified in the 16 species obtained from MycoCosm,
501 3 isolates of *M. pernicioso* (C-BA3, S-MG3, L-EC1, one representing each biotype), an isolate of
502 *M. roreri* (R-CO1), and PRY1 of *S. cerevisiae* as the outgroup. To improve alignment quality,
503 trimAl package (Capella-Gutiérrez et al., 2009) was used. For dN/dS analysis, considering each
504 gene family independently, the phylogenetic reconstruction was performed using IQ-Tree (v.
505 1.6.6) with the multiple local alignment of the protein sequences obtained with Mafft (v.
506 7.407), and the codon-based alignment of the nucleotide sequences was performed with
507 Macse (v. 2.01) (Ranwez et al., 2018).

508

509 **Detection of positive selection signals**

510 To search for genes and regions that are potentially under positive selection in each
511 of the PR-1 families of the 22 isolates, the CodeML program of the PAML 4.7 package (Yang,
512 2007) was used with the ETEToolkit tool (Huerta-Cepas et al., 2016). CodeML implements a
513 modification of the model proposed by (Goldman & Yang, 1994) to calculate the omega (rate
514 of non-synonymous mutations (dN)/rate of synonymous mutations (dS)) of a coding gene

515 from the multiple alignment sequences and phylogenetic relationships that have been
516 previously inferred.

517 In order to detect positive selection signals in isolates or specific positions in the
518 sequences, we performed tests with the “branch-site” model, which compares a null model
519 (bsA1) in which the branch under consideration is evolving without restrictions ($dN/dS = 1$)
520 against a model in which the same branch has sites evolving under positive selection (bsA)
521 ($dN/dS > 1$) (Zhang et al., 2005). In these tests, those branches that were tested for significantly
522 different evolving rates from the others (foreground branches ω_{frg}) are marked in the
523 phylogenetic trees – in this case, the branches corresponding to the isolates of the C-biotype
524 or S-biotype. To detect signs of positive selection at specific sites throughout the sequences,
525 regardless of the isolate, we used the “sites” model (M2 and M1, NSsites 0 1 2) to test all
526 branches of the phylogenetic trees.

527 In both tests, the models are executed several times with different initial omegas (0.2,
528 0.7, 1.2), and the models with the highest probability are selected for the hypothesis test, in
529 which a comparison between the alternative model and the null model is made through a
530 likelihood ratio test. If the alternative model is the most likely one (p-value < 0.05), then the
531 possibility of positive selection ($\omega > 1$) can be accepted, and sites with evidence of selection
532 (probability > 0.95) are reported by Bayes Empirical Bayes analysis (BEB) (Zhang et al., 2005).
533

534 **Gene amplification and synteny analysis of *PR-1c***

535 In order to confirm the presence or absence of *MpPR-1c* and *MpPR-1d* genes in the
536 genomes of *M. perniciosa* isolates, these genes were amplified by polymerase chain reaction
537 (PCR) from isolates C-AC1, C-BA1a, C-BA3, S-AM1, S-MG3, S-MG4, L-EC1 and L-EC2. The
538 necrotrophic mycelia of these isolates was cultivated in 1.7% MYEA media (15 g L⁻¹ agar; 5 g
539 L⁻¹ yeast extract, 17 g L⁻¹ malt extract) at 28°C for 14 days, then harvested and ground in liquid
540 nitrogen for total DNA isolation with the phenol-chloroform method (Sambrook & Russell,
541 2006). PCRs were performed with primers designed for *MpPR-1c* (F: 5'-
542 GGATCCCGACTTGACAACCTCCATCTCG-3', R: 5'-GAGCTCTCACTCAAACCTCCCGTCATAAT-3')
543 and *MpPR-1d* (F: 5'-GGATCCCCCTCGCAATGGGTTTTTC-3', R: 5'-
544 GTCGACTCAGTCAAGATCAGCCTGGAGA-3') and amplifications cycles consisting of an initial
545 stage of 94°C for 3 min, 35 cycles of 95°C for 30s, 60°C for 50 s and 72°C for 1 min, and final
546 extension at 72°C for 10 min.

547 For synteny analysis, the positions of *PR-1j*, *PR-1c* and *PR-1d* genes were searched in
548 the scaffolds of genomes C-BA3, S-MG2, R-CO2, L-EC1 and L-EC2 by blastn. The scaffolds were
549 then excised 5000bp upstream and 5000bp downstream from the starting position of *PR-1j* in
550 the scaffolds. The resulting 10000 bp excised scaffolds were used for synteny analysis with
551 Mummer (v. 4.0.0beta2) (Kurtz et al., 2004), using the C-BA3 sequence as the reference.

552

553 ***MpPR-1* expression data**

554 *MpPR-1* expression data in RPKM (Reads Per Kilobase per Million mapped reads)
555 values from the C-biotype of *M. perniciosa* in seven biological conditions (dikaryotic mycelium
556 14 days, basidiomata, germinating spores, green broom, initial necrosis, advanced necrosis,
557 dry broom) were downloaded from the Witches' Broom Disease Transcriptome Atlas (v. 1.1)
558 (<http://bioinfo08.ibi.unicamp.br/atlas/>).

559 *MpPR-1* expression data of *M. perniciosa* treated with plant antifungal compounds
560 were obtained from RNA-seq data. The C-BA1a isolate's necrotrophic mycelia was initially
561 inoculated in 100 mL of liquid MYEA media and cultivated for 5 days under agitation of 150
562 rpm at 30°C, then 5 mL of this initial cultivation were transferred to 50 mL of fresh MYEA
563 liquid media containing eugenol (500µM), α -tomatin (80µM) or DMSO (250 µL, solvent
564 control) and cultivated again under agitation of 150 rpm at 30°C for 7 days. The total RNA was
565 extracted using the Rneasy® Plant Mini Kit (Quiagen, USA) and quantified on a fluorimeter
566 (Qubit, Invitrogen). cDNA libraries were prepared in five biological replicates for each
567 treatment, plus biological control. The cDNA libraries were built from 1000 ng of total RNA
568 using Illumina's TruSeq RNA Sample Prep kit, as recommended by the manufacturer. The
569 libraries were prepared according to Illumina's standard procedure and sequenced on
570 Illumina's HiSeq 2500 sequencer. The quality of raw sequences was assessed with FastQC
571 (v.0.11.7). Read quantification was performed by mapping the generated reads against 16084
572 gene models of the C-BA1a genome using Salmon (v.0.14.1) in mapping-based mode (Patro et
573 al., 2017). Read counts were normalized to Transcripts Per Million (TPM) values for plotting.
574 Differential expression analysis was performed with the DESeq2 (v.1.22.2) package using
575 Wald test and Log fold change shrinkage by the *apecglm* method (IfcThreshold=0.1, s-value
576 <0.005) (Love et al., 2014). TPM values and DESeq2 results for *MpPR-1* genes in these
577 experimental conditions are available at Supplementary Table 2.

578 *MpPR-1* expression data in TPM for the S-biotype was obtained from RNA-seq libraries
579 of infected MicroTom tomato plants in 7 different time points after inoculation (12h, 24h, 48h,
580 5 days, 10 days, 20 days, 30 days) (Costa et al., under review). The quality of raw sequences
581 was assessed with FastQC (v. 0.11.7). Next, Trimmomatic (v.0.36) (Bolger et al., 2014) was used
582 to remove adaptor-containing and low-quality sequences. Quality-filtered reads were then
583 aligned against the S-MG1 or S-MG2 reference genome using HISAT2 (v.2.1.0) with default
584 parameters (Kim et al., 2019). Reads that mapped to coding sequences were counted with
585 featureCounts (v.1.6.3) (Liao et al., 2014). TPM values for *MpPR-1* genes in these experimental
586 conditions are available at Supplementary Table 3.

587 *MrPR-1* expression data in TPM was obtained from RNA-Seq reads of *M. roreri* in the
588 biotrophic (30 days after infection) and necrotrophic (60 days after infection) stages of frosty
589 pod rot from (Meinhardt et al., 2014). Reads were mapped and quantified with Salmon
590 (v.0.14.1) (Patro et al., 2017) using 17910 gene models of *M. roreri* MCA 2997 (GCA_000488995)
591 available at Ensembl Fungi.

592

593 **Funding**

594 This work was supported by the São Paulo Research Foundation (FAPESP) grants to
595 M.F.C (#2013/08293-7), P.J.P.L.T. (#2009/51018-1) and G.A.G.P. (#2016/10498-4), and FAPESP
596 fellowships to A.A.V (#2017/13015-7), A.P.C. (#2018/04240-0), G.L.F (#2011/23315-1,
597 #2013/09878-9, #2014/06181-0), P.F.V.P. (#2013/05979-5, #2014/00802-2) and R.M.B
598 (#2017/13319-6).

599

600 **Acknowledgements**

601 We are thankful to Msc. Bárbara A. Pires and Dr. Mario O. Barsottini for helping with
602 the experiments with *M. perniciosa* treated with antifungal compounds and Msc. Leandro C.
603 do Nascimento for performing the assembly of *Moniliophthora* genomes.

604

605 **Competing interests**

606 The authors declare no competing interests.

607

608 **Author contributions**

609 J.J. and R.M.B. conceived and supervised this project. A.A.V. performed identification
610 of PR-1-like candidate genes, evolutionary analysis, and most expression analysis from RNA-
611 seq data, executed PCR experiments and generated figures. P.J.P.L.T. and D.P.T.T. conceived
612 the project of genomics of *Moniliophthora* isolates. P.J.P.L.T., D.P.T.T., P.F.V.P. and G.L.F.
613 executed genomic data acquisition of *Moniliophthora* isolates. P.J.P.L.T. analyzed RNA-Seq
614 libraries of MT plants infected with S-biotype. P.M.T.F. performed gene prediction,
615 annotation, and assignment of orthogroups from genomes. A. P. C. helped with genomic and
616 RNA-seq analysis. R.M.B. conceived and executed RNA-seq data acquisition of *M. perniciosa*
617 treated with antifungal compounds and A.A.V. analyzed this data. A.A.V. and J.J. wrote the
618 original draft. J.J. and A.P.C. improved the design of figures. J.J., R.M.B, P.J.P.L.T, D.P.T.T.,
619 G.L.F., A.P.C., P.F.V.P. and G.A.G.P. reviewed and edited the draft. M.F.C. and G.A.G.P.
620 contributed with project supervision and funding acquisition. All authors read and approved
621 the final manuscript.

622

623 **References**

- 624 Aime, M. C., & Phillips-Mora, W. (2005). The causal agents of witches' broom and frosty pod
625 rot of cacao (chocolate, *Theobroma cacao*) form a new lineage of Marasmiaceae.
626 *Mycologia*, 97(5), 1012–1022. <https://doi.org/10.3852/mycologia.97.5.1012>
- 627 Asojo, O. A., Goud, G., Dhar, K., Loukas, A., Zhan, B., Deumic, V., Liu, S., Borgstahl, G. E.
628 O., & Hotez, P. J. (2005). X-ray structure of Na-ASP-2, a pathogenesis-related-1
629 protein from the nematode parasite, *Necator americanus*, and a vaccine antigen for
630 human hookworm infection. *Journal of Molecular Biology*, 346(3), 801–814.
631 <https://doi.org/10.1016/j.jmb.2004.12.023>
- 632 Baroni, R. M., Luo, Z., Darwiche, R., Hudspeth, E. M., Schneiter, R., Pereira, G. A. G.,
633 Mondego, J. M. C., & Asojo, O. A. (2017). Crystal Structure of MpPR-1i, a SCP/TAPS
634 protein from *Moniliophthora perniciosa*, the fungus that causes Witches' Broom
635 Disease of Cacao. *Scientific Reports*, 7(1), 7818. <https://doi.org/10.1038/s41598-017-07887-1>
- 637 Bolger, A. M., Lohse, M., & Usadel, B. (2014). Trimmomatic: A flexible trimmer for Illumina
638 sequence data. *Bioinformatics*, 30(15), 2114–2120.
639 <https://doi.org/10.1093/bioinformatics/btu170>
- 640 Braun, B. R., Head, W. S., Wang, M. X., & Johnson, A. D. (2000). Identification and
641 characterization of TUP1-regulated genes in *Candida albicans*. *Genetics*, 156(1), 31–
642 44.
- 643 Butler, G., Rasmussen, M. D., Lin, M. F., Santos, M. A. S., Sakthikumar, S., Munro, C. A.,
644 Rheinbay, E., Grabherr, M., Forche, A., Reedy, J. L., Agrafioti, I., Arnaud, M. B.,
645 Bates, S., Brown, A. J. P., Brunke, S., Costanzo, M. C., Fitzpatrick, D. A., de Groot, P.
646 W. J., Harris, D., ... Cuomo, C. A. (2009). Evolution of pathogenicity and sexual
647 reproduction in eight *Candida* genomes. *Nature*, 459(7247), 657–662.
648 <https://doi.org/10.1038/nature08064>

- 649 Camacho, C., Coulouris, G., Avagyan, V., Ma, N., Papadopoulos, J., Bealer, K., & Madden, T.
650 L. (2009). BLAST+: Architecture and applications. *BMC Bioinformatics*, 10(1), 421.
651 <https://doi.org/10.1186/1471-2105-10-421>
- 652 Cantacessi, C., Campbell, B. E., Visser, A., Geldhof, P., Nolan, M. J., Nisbet, A. J., Matthews,
653 J. B., Loukas, A., Hofmann, A., Otranto, D., Sternberg, P. W., & Gasser, R. B. (2009).
654 A portrait of the “SCP/TAPS” proteins of eukaryotes—Developing a framework for
655 fundamental research and biotechnological outcomes. *Biotechnology Advances*, 27(4),
656 376–388. <https://doi.org/10.1016/j.biotechadv.2009.02.005>
- 657 Capella-Gutiérrez, S., Silla-Martínez, J. M., & Gabaldón, T. (2009). trimAl: A tool for
658 automated alignment trimming in large-scale phylogenetic analyses. *Bioinformatics*
659 (*Oxford, England*), 25(15), 1972–1973. <https://doi.org/10.1093/bioinformatics/btp348>
- 660 Chalmers, I. W., McArdle, A. J., Coulson, R. M., Wagner, M. A., Schmid, R., Hirai, H., &
661 Hoffmann, K. F. (2008). Developmentally regulated expression, alternative splicing
662 and distinct sub-groupings in members of the *Schistosoma mansoni* venom allergen-
663 like (SmVAL) gene family. *BMC Genomics*, 9(1), 89. [https://doi.org/10.1186/1471-2164-](https://doi.org/10.1186/1471-2164-9-89)
664 9-89
- 665 Chen, Y.-L., Lee, C.-Y., Cheng, K.-T., Chang, W.-H., Huang, R.-N., Nam, H. G., & Chen, Y.-R.
666 (2014). Quantitative Peptidomics Study Reveals That a Wound-Induced Peptide from
667 PR-1 Regulates Immune Signaling in Tomato. *The Plant Cell*, 26(10), 4135–4148.
668 <https://doi.org/10.1105/tpc.114.131185>
- 669 Chien, P.-S., Nam, H. G., & Chen, Y.-R. (2015). A salt-regulated peptide derived from the CAP
670 superfamily protein negatively regulates salt-stress tolerance in *Arabidopsis*. *Journal*
671 *of Experimental Botany*, 66(17), 5301–5313. <https://doi.org/10.1093/jxb/erv263>
- 672 Choudhary, V., & Schneider, R. (2012). Pathogen-Related Yeast (PRY) proteins and members
673 of the CAP superfamily are secreted sterol-binding proteins. *Proceedings of the*
674 *National Academy of Sciences of the United States of America*, 109(42), 16882–16887.
675 <https://doi.org/10.1073/pnas.1209086109>
- 676 Darwiche, R., El Atab, O., Baroni, R. M., Teixeira, P. J. P. L., Mondego, J. M. C., Pereira, G.
677 A. G., & Schneider, R. (2017). Plant pathogenesis-related proteins of the cacao fungal
678 pathogen *Moniliophthora perniciosa* differ in their lipid-binding specificities. *The*
679 *Journal of Biological Chemistry*, 292(50), 20558–20569.
680 <https://doi.org/10.1074/jbc.M117.811398>
- 681 Darwiche, R., Mène-Saffrané, L., Gfeller, D., Asojo, O. A., & Schneider, R. (2017). The
682 pathogen-related yeast protein Pry1, a member of the CAP protein superfamily, is a
683 fatty acid-binding protein. *The Journal of Biological Chemistry*, 292(20), 8304–8314.
684 <https://doi.org/10.1074/jbc.M117.781880>
- 685 Darwiche, R., & Schneider, R. (2016). Cholesterol-Binding by the Yeast CAP Family Member
686 Pry1 Requires the Presence of an Aliphatic Side Chain on Cholesterol. *Journal of*
687 *Steroids & Hormonal Science*, 7(2). <https://doi.org/10.4172/2157-7536.1000172>
- 688 Deganello, J., Leal, G. A., Rossi, M. L., Peres, L. E. P., & Figueira, A. (2014). Interaction of
689 *Moniliophthora perniciosa* biotypes with Micro-Tom tomato: A model system to
690 investigate the witches’ broom disease of *Theobroma cacao*. *Plant Pathology*, 63(6),
691 1251–1263. <https://doi.org/10.1111/ppa.12206>
- 692 Ding, X., Shields, J., Allen, R., & Hussey, R. S. (2000). Molecular cloning and
693 characterisation of a venom allergen AG5-like cDNA from *Meloidogyne incognita*.
694 *International Journal for Parasitology*, 30(1), 77–81. [https://doi.org/10.1016/s0020-](https://doi.org/10.1016/s0020-7519(99)00165-4)
695 7519(99)00165-4
- 696 Eddy, S. R. (2011). Accelerated Profile HMM Searches. *PLoS Computational Biology*, 7(10),
697 e1002195. <https://doi.org/10.1371/journal.pcbi.1002195>
- 698 Emms, D. M., & Kelly, S. (2015). OrthoFinder: Solving fundamental biases in whole genome

- 699 comparisons dramatically improves orthogroup inference accuracy. *Genome Biology*,
700 16(1), 157. <https://doi.org/10.1186/s13059-015-0721-2>
- 701 Evans, H. C. (1978). Witches' broom disease of cocoa *Crinipellis pernicios* in Ecuador.
702 *Annals of Applied Biology*, 89(2), 185–192. <https://doi.org/10.1111/j.1744->
703 7348.1978.tb07689.x
- 704 Evans, Harry C. (2007). Cacao Diseases—The Trilogy Revisited. *Phytopathology*[®], 97(12),
705 1640–1643. <https://doi.org/10.1094/PHYTO-97-12-1640>
- 706 Fedorova, N. D., Khaldi, N., Joardar, V. S., Maiti, R., Amedeo, P., Anderson, M. J., Crabtree,
707 J., Silva, J. C., Badger, J. H., Albarraq, A., Angiuoli, S., Bussey, H., Bowyer, P., Cotty,
708 P. J., Dyer, P. S., Egan, A., Galens, K., Fraser-Liggett, C. M., Haas, B. J., ... Nierman,
709 W. C. (2008). Genomic Islands in the Pathogenic Filamentous Fungus *Aspergillus*
710 *fumigatus*. *PLOS Genetics*, 4(4), e1000046.
711 <https://doi.org/10.1371/journal.pgen.1000046>
- 712 Fiorin, G. L., Sánchez-Vallet, A., Thomazella, D. P. de T., do Prado, P. F. V., do Nascimento,
713 L. C., Figueira, A. V. de O., Thomma, B. P. H. J., Pereira, G. A. G., & Teixeira, P. J. P.
714 L. (2018). Suppression of Plant Immunity by Fungal Chitinase-like Effectors. *Current*
715 *Biology: CB*, 28(18), 3023-3030.e5. <https://doi.org/10.1016/j.cub.2018.07.055>
- 716 Gamir, J., Darwiche, R., Van't Hof, P., Choudhary, V., Stumpe, M., Schneiter, R., & Mauch,
717 F. (2017). The sterol-binding activity of PATHOGENESIS-RELATED PROTEIN 1
718 reveals the mode of action of an antimicrobial protein. *The Plant Journal: For Cell and*
719 *Molecular Biology*, 89(3), 502–509. <https://doi.org/10.1111/tpj.13398>
- 720 Gao, B., Allen, R., Maier, T., Davis, E. L., Baum, T. J., & Hussey, R. S. (2001). Molecular
721 characterisation and expression of two venom allergen-like protein genes in
722 *Heterodera glycines*. *International Journal for Parasitology*, 31(14), 1617–1625.
723 [https://doi.org/10.1016/s0020-7519\(01\)00300-9](https://doi.org/10.1016/s0020-7519(01)00300-9)
- 724 Gibbs, G. M., Roelants, K., & O'Bryan, M. K. (2008). The CAP superfamily: Cysteine-rich
725 secretory proteins, antigen 5, and pathogenesis-related 1 proteins--roles in
726 reproduction, cancer, and immune defense. *Endocrine Reviews*, 29(7), 865–897.
727 <https://doi.org/10.1210/er.2008-0032>
- 728 Goldman, N., & Yang, Z. (1994). A codon-based model of nucleotide substitution for protein-
729 coding DNA sequences. *Molecular Biology and Evolution*, 11(5), 725–736.
730 <https://doi.org/10.1093/oxfordjournals.molbev.a040153>
- 731 Griffith, G. W., & Hedger, J. N. (1994). Spatial distribution of mycelia of the liana (L-) biotype
732 of the agaric *Crinipellis pernicios* (Stahel) Singer in tropical forest. *New Phytologist*,
733 127(2), 243–259. <https://doi.org/10.1111/j.1469-8137.1994.tb04276.x>
- 734 Grigoriev, I. V., Nikitin, R., Haridas, S., Kuo, A., Ohm, R., Otilar, R., Riley, R., Salamov, A.,
735 Zhao, X., Korzeniewski, F., Smirnova, T., Nordberg, H., Dubchak, I., & Shabalov, I.
736 (2014). MycoCosm portal: Gearing up for 1000 fungal genomes. *Nucleic Acids*
737 *Research*, 42(Database issue), D699-704. <https://doi.org/10.1093/nar/gkt1183>
- 738 Hawdon, J. M., Narasimhan, S., & Hotez, P. J. (1999). Ancylostoma secreted protein 2:
739 Cloning and characterization of a second member of a family of nematode secreted
740 proteins from *Ancylostoma caninum*. *Molecular and Biochemical Parasitology*, 99(2),
741 149–165. [https://doi.org/10.1016/s0166-6851\(99\)00011-0](https://doi.org/10.1016/s0166-6851(99)00011-0)
- 742 Huerta-Cepas, J., Serra, F., & Bork, P. (2016). ETE 3: Reconstruction, Analysis, and
743 Visualization of Phylogenomic Data. *Molecular Biology and Evolution*, 33(6), 1635–
744 1638. <https://doi.org/10.1093/molbev/msw046>
- 745 Hunter, S., Apweiler, R., Attwood, T. K., Bairoch, A., Bateman, A., Binns, D., Bork, P., Das,
746 U., Daugherty, L., Duquenne, L., Finn, R. D., Gough, J., Haft, D., Hulo, N., Kahn, D.,
747 Kelly, E., Laugraud, A., Letunic, I., Lonsdale, D., ... Yeats, C. (2009). InterPro: The
748 integrative protein signature database. *Nucleic Acids Research*, 37(Database issue),

- 749 D211–D215. <https://doi.org/10.1093/nar/gkn785>
- 750 Kasparovsky, T., Milat, M.-L., Humbert, C., Blein, J.-P., Havel, L., & Mikes, V. (2003).
751 Elicitation of tobacco cells with ergosterol activates a signal pathway including
752 mobilization of internal calcium. *Plant Physiology and Biochemistry*, *41*(5), 495–501.
753 [https://doi.org/10.1016/S0981-9428\(03\)00058-5](https://doi.org/10.1016/S0981-9428(03)00058-5)
- 754 Katoh, K., & Standley, D. M. (2013). MAFFT Multiple Sequence Alignment Software Version
755 7: Improvements in Performance and Usability. *Molecular Biology and Evolution*,
756 *30*(4), 772–780. <https://doi.org/10.1093/molbev/mst010>
- 757 Kelleher, A., Darwiche, R., Rezende, W. C., Farias, L. P., Leite, L. C. C., Schneider, R., &
758 Asojo, O. A. (2014). Schistosoma mansoni venom allergen-like protein 4 (SmVAL4) is
759 a novel lipid-binding SCP/TAPS protein that lacks the prototypical CAP motifs. *Acta*
760 *Crystallographica Section D: Biological Crystallography*, *70*(Pt 8), 2186–2196.
761 <https://doi.org/10.1107/S1399004714013315>
- 762 Kerekes, J., Desjardin, D., & Desjardin, D. (2009). A monograph of the genera Crinipellis and
763 Moniliophthora from Southeast Asia including a molecular phylogeny of the nrITS
764 region. *Fungal Diversity*, *37*, 101–152.
- 765 Khoza, T. G., Dubery, I. A., & Piater, L. A. (2019). Identification of Candidate Ergosterol-
766 Responsive Proteins Associated with the Plasma Membrane of Arabidopsis thaliana.
767 *International Journal of Molecular Sciences*, *20*(6). <https://doi.org/10.3390/ijms20061302>
- 768 Kim, D., Paggi, J. M., Park, C., Bennett, C., & Salzberg, S. L. (2019). Graph-based genome
769 alignment and genotyping with HISAT2 and HISAT-genotype. *Nature Biotechnology*,
770 *37*(8), 907–915. <https://doi.org/10.1038/s41587-019-0201-4>
- 771 Klemptner, R. L., Sherwood, J. S., Tugizimana, F., Dubery, I. A., & Piater, L. A. (2014).
772 Ergosterol, an orphan fungal microbe-associated molecular pattern (MAMP).
773 *Molecular Plant Pathology*, *15*(7), 747–761. <https://doi.org/10.1111/mpp.12127>
- 774 Kropp, B. R., & Albee-Scott, S. (2012). Moniliophthora aurantiaca sp. Nov., a Polynesian
775 species occurring in littoral forests. *Mycotaxon*, *120*(1), 493–503.
776 <https://doi.org/10.5248/120.493>
- 777 Kurtz, S., Phillippy, A., Delcher, A. L., Smoot, M., Shumway, M., Antonescu, C., & Salzberg,
778 S. L. (2004). Versatile and open software for comparing large genomes. *Genome*
779 *Biology*, *5*(2), R12. <https://doi.org/10.1186/gb-2004-5-2-r12>
- 780 Lemoine, F., Domelevo Entfellner, J.-B., Wilkinson, E., Correia, D., Dávila Felipe, M., De
781 Oliveira, T., & Gascuel, O. (2018). Renewing Felsenstein’s phylogenetic bootstrap in
782 the era of big data. *Nature*, *556*(7702), 452–456. [https://doi.org/10.1038/s41586-018-](https://doi.org/10.1038/s41586-018-0043-0)
783 [0043-0](https://doi.org/10.1038/s41586-018-0043-0)
- 784 Liao, Y., Smyth, G. K., & Shi, W. (2014). featureCounts: An efficient general purpose
785 program for assigning sequence reads to genomic features. *Bioinformatics*, *30*(7),
786 923–930. <https://doi.org/10.1093/bioinformatics/btt656>
- 787 Lochman, J., & Mikes, V. (2006). Ergosterol treatment leads to the expression of a specific
788 set of defence-related genes in tobacco. *Plant Molecular Biology*, *62*(1–2), 43–51.
789 <https://doi.org/10.1007/s11103-006-9002-5>
- 790 Love, M. I., Huber, W., & Anders, S. (2014). Moderated estimation of fold change and
791 dispersion for RNA-seq data with DESeq2. *Genome Biology*, *15*(12).
792 <https://doi.org/10.1186/s13059-014-0550-8>
- 793 Lozano-Torres, J. L., Wilbers, R. H. P., Warmerdam, S., Finkers-Tomczak, A., Diaz-
794 Granados, A., van Schaik, C. C., Helder, J., Bakker, J., Goverse, A., Schots, A., &
795 Smant, G. (2014). Apoplactic venom allergen-like proteins of cyst nematodes
796 modulate the activation of basal plant innate immunity by cell surface receptors.
797 *PLoS Pathogens*, *10*(12), e1004569. <https://doi.org/10.1371/journal.ppat.1004569>
- 798 Manel, S., Perrier, C., Pratlong, M., Abi-Rached, L., Paganini, J., Pontarotti, P., & Aurelle, D.

- 799 (2016). Genomic resources and their influence on the detection of the signal of
800 positive selection in genome scans. *Molecular Ecology*, 25(1), 170–184.
801 <https://doi.org/10.1111/mec.13468>
- 802 Meinhardt, L. W., Costa, G. G. L., Thomazella, D. P., Teixeira, P. J. P., Carazzolle, M. F.,
803 Schuster, S. C., Carlson, J. E., Guiltinan, M. J., Mieczkowski, P., Farmer, A., Ramaraj,
804 T., Crozier, J., Davis, R. E., Shao, J., Melnick, R. L., Pereira, G. A., & Bailey, B. A.
805 (2014). Genome and secretome analysis of the hemibiotrophic fungal pathogen,
806 *Moniliophthora roreri*, which causes frosty pod rot disease of cacao: Mechanisms of
807 the biotrophic and necrotrophic phases. *BMC Genomics*, 15(1), 164.
808 <https://doi.org/10.1186/1471-2164-15-164>
- 809 Mohd As'wad, A. W., Sariah, M., Paterson, R. R. M., Zainal Abidin, M. A., & Lima, N. (2011).
810 Ergosterol analyses of oil palm seedlings and plants infected with *Ganoderma*. *Crop*
811 *Protection*, 30(11), 1438–1442. <https://doi.org/10.1016/j.cropro.2011.07.004>
- 812 Nguyen, L.-T., Schmidt, H. A., von Haeseler, A., & Minh, B. Q. (2015). IQ-TREE: A fast and
813 effective stochastic algorithm for estimating maximum-likelihood phylogenies.
814 *Molecular Biology and Evolution*, 32(1), 268–274.
815 <https://doi.org/10.1093/molbev/msu300>
- 816 Niveiro, N., Ramírez, N. A., Michlig, A., Lodge, D. J., & Aime, M. C. (2020). Studies of
817 Neotropical tree pathogens in *Moniliophthora*: A new species, *M. mayarum*, and
818 new combinations for *Crinipellis ticoi* and *C. brasiliensis*. *MycKeys*, 66, 39–54.
819 <https://doi.org/10.3897/mycokeys.66.48711>
- 820 Nürnberger, T., Brunner, F., Kemmerling, B., & Piater, L. (2004). Innate immunity in plants
821 and animals: Striking similarities and obvious differences. *Immunological Reviews*,
822 198, 249–266. <https://doi.org/10.1111/j.0105-2896.2004.0119.x>
- 823 Oleksyk, T. K., Smith, M. W., & O'Brien, S. J. (2010). Genome-wide scans for footprints of
824 natural selection. *Philosophical Transactions of the Royal Society B: Biological Sciences*,
825 365(1537), 185–205. <https://doi.org/10.1098/rstb.2009.0219>
- 826 Patro, R., Duggal, G., Love, M. I., Irizarry, R. A., & Kingsford, C. (2017). Salmon provides fast
827 and bias-aware quantification of transcript expression. *Nature Methods*, 14(4), 417–
828 419. <https://doi.org/10.1038/nmeth.4197>
- 829 Prados-Rosales, R. C., Roldán-Rodríguez, R., Serena, C., López-Berges, M. S., Guarro, J.,
830 Martínez-del-Pozo, Á., & Di Pietro, A. (2012). A PR-1-like Protein of *Fusarium*
831 *oxysporum* Functions in Virulence on Mammalian Hosts. *The Journal of Biological*
832 *Chemistry*, 287(26), 21970–21979. <https://doi.org/10.1074/jbc.M112.364034>
- 833 Purdy, L., & Schmidt, R. (1996). STATUS OF CACAO WITCHES' BROOM: Biology,
834 Epidemiology, and Management. *Annual Review of Phytopathology*, 34(1), 573–594.
835 <https://doi.org/10.1146/annurev.phyto.34.1.573>
- 836 Ranwez, V., Douzery, E. J. P., Cambon, C., Chantret, N., & Delsuc, F. (2018). MACSE v2:
837 Toolkit for the Alignment of Coding Sequences Accounting for Frameshifts and Stop
838 Codons. *Molecular Biology and Evolution*, 35(10), 2582–2584.
839 <https://doi.org/10.1093/molbev/msy159>
- 840 Sambrook, J., & Russell, D. W. (2006). Purification of nucleic acids by extraction with
841 phenol:chloroform. *CSH Protocols*, 2006(1). <https://doi.org/10.1101/pdb.prot4455>
- 842 Schneider, R., & Di Pietro, A. (2013). The CAP protein superfamily: Function in sterol export
843 and fungal virulence. *Biomolecular Concepts*, 4(5), 519–525.
844 <https://doi.org/10.1515/bmc-2013-0021>
- 845 Takahashi, H. (2002). Four new species of *Crinipellis* and *Marasmius* in eastern Honshu,
846 Japan. *Mycoscience*, 43(4), 343–350. <https://doi.org/10.1007/S102670200050>
- 847 Teixeira, Paulo J. P. L., Thomazella, D. P. T., Vidal, R. O., do Prado, P. F. V., Reis, O., Baroni,
848 R. M., Franco, S. F., Mieczkowski, P., Pereira, G. A. G., & Mondego, J. M. C. (2012).

- 849 The fungal pathogen *Moniliophthora perniciosa* has genes similar to plant PR-1 that
850 are highly expressed during its interaction with cacao. *PLoS One*, 7(9), e45929.
851 <https://doi.org/10.1371/journal.pone.0045929>
- 852 Teixeira, Paulo José Pereira Lima, Costa, G. G. L., Fiorin, G. L., Pereira, G. A. G., &
853 Mondego, J. M. C. (2013). Novel receptor-like kinases in cacao contain PR-1
854 extracellular domains. *Molecular Plant Pathology*, 14(6), 602–609.
855 <https://doi.org/10.1111/mpp.12028>
- 856 Teixeira, Paulo José Pereira Lima, Thomazella, D. P. de T., & Pereira, G. A. G. (2015). Time
857 for Chocolate: Current Understanding and New Perspectives on Cacao Witches'
858 Broom Disease Research. *PLoS Pathogens*, 11(10).
859 <https://doi.org/10.1371/journal.ppat.1005130>
- 860 Teixeira, Paulo José Pereira Lima, Thomazella, D. P. de T., Reis, O., Prado, P. F. V. do, Rio,
861 M. C. S. do, Fiorin, G. L., José, J., Costa, G. G. L., Negri, V. A., Mondego, J. M. C.,
862 Mieczkowski, P., & Pereira, G. A. G. (2014). High-Resolution Transcript Profiling of
863 the Atypical Biotrophic Interaction between *Theobroma cacao* and the Fungal
864 Pathogen *Moniliophthora perniciosa*. *The Plant Cell*, 26(11), 4245–4269.
865 <https://doi.org/10.1105/tpc.114.130807>
- 866 van Loon, L. C., Rep, M., & Pieterse, C. M. J. (2006). Significance of inducible defense-
867 related proteins in infected plants. *Annual Review of Phytopathology*, 44, 135–162.
868 <https://doi.org/10.1146/annurev.phyto.44.070505.143425>
- 869 Yang, Z. (2007). PAML 4: Phylogenetic analysis by maximum likelihood. *Molecular Biology*
870 *and Evolution*, 24(8), 1586–1591. <https://doi.org/10.1093/molbev/msm088>
- 871 Zhan, B., Liu, Y., Badamchian, M., Williamson, A., Feng, J., Loukas, A., Hawdon, J. M., &
872 Hotez, P. J. (2003). Molecular characterisation of the *Ancylostoma*-secreted protein
873 family from the adult stage of *Ancylostoma caninum*. *International Journal for*
874 *Parasitology*, 33(9), 897–907. [https://doi.org/10.1016/s0020-7519\(03\)00111-5](https://doi.org/10.1016/s0020-7519(03)00111-5)
- 875 Zhang, J., Nielsen, R., & Yang, Z. (2005). Evaluation of an Improved Branch-Site Likelihood
876 Method for Detecting Positive Selection at the Molecular Level. *Molecular Biology and*
877 *Evolution*, 22(12), 2472–2479. <https://doi.org/10.1093/molbev/msi237>
- 878 Zhao, X. R., Lin, Q., & Brookes, P. C. (2005). Does soil ergosterol concentration provide a
879 reliable estimate of soil fungal biomass? *Soil Biology and Biochemistry*, 37(2), 311–317.
880 <https://doi.org/10.1016/j.soilbio.2004.07.041>